Chapter 12
COSY

David M. Doddrell

Centre for Magnetic Resonance, University of Queensland, 4072, Australia

12.1 INTRODUCTION

Although conceivably the simplest two-dimensional (2D) experiment possible, the physics underpinning the COSY (homonuclear correlated spectroscopy) experiment[1] are often the most difficult for the non-NMR specialist to grasp. The reason for this difficulty is undoubtedly the reluctance of many NMR users to grapple with the basics of product-operator algebra.[2] It is a fact that although some features of NMR experiments (for example, signal generation, the formation of a spin echo, and so on) can be understood using vector arguments, these arguments do not translate simply to 2D spectroscopy. With this statement in mind, it is assumed that the interested reader of this article is familiar with product operator algebra before any attempt is made to understand the nuances of the COSY experiment.

Before proceeding further, there is one important fact to note concerning the detection of NMR signals in general. Quadrature detection is employed in NMR spectroscopy to distinguish between resonances whose frequencies are either positive or negative relative to the reference frequency, usually the same frequency at which the rf pulses are applied. The reference frequency defines the rotating frame frequency. Thus, in this frame of reference, any precession of the spins that resonate at the reference frequency (the on-resonance condition) is zero and their decay as measured by the receiver is that of a pure exponential with a decay time T_2^*. The signal acquired by the U channel of the receiver is proportional to $I_x \cos \Delta\omega t_2$, where $\Delta\omega$ is the offset frequency from the reference and the signal has been acquired for a time t_2. Because $\cos x = \cos(-x)$, positive and negative frequencies are not distinguished by single channel reception. If a second channel, the V channel, is used to receive signals but its reference frequency is phase shifted by 90°, the signal acquired is proportional to $I_y \sin \Delta\omega t_2$. If the signals from the two channels are combined, the combined signal is proportional to $I_x \cos \Delta\omega t_2 + I_y \sin \Delta\omega t_2$. This can be written as $I_x \exp(-\mathrm{i}\Delta\omega t_2)$ using the Liouville space transformation between I_x and I_y; $I_y = -\mathrm{i}I_x$. The term $I_x \exp(-\mathrm{i}\Delta\omega t_2)$ thus represents a single resonance appearing at $-\Delta\omega$.

12.2 THE COSY EXPERIMENT

12.2.1 Product Operator Algebra for the Basic Pulse Sequence

The basic COSY pulse sequence is

$$\frac{\pi}{2}(i),\ t_1,\ \frac{\pi}{2}(j),\ \text{acquire for time } t_2 \qquad (12.1)$$

where i and j are the phases of the applied rf pulses. Consider the application of this pulse sequence to a homonuclear spin-coupled system, *IS*. Assume that the weak coupling approximation — $(\Delta\omega_I - \Delta\omega_S) \gg 2\pi J$ — is valid, where J is the scalar I–S coupling constant and $\Delta\omega_I$ and $\Delta\omega_S$ are the frequency offsets of the I and S spins in the rotating frame, respectively.

The initial spin coherences prior to the application of the pulse sequence are $I_z U^S$ and $U^I S_z$, respectively, where U is the identity operator. The first pulse with phase $i = x$ induces the following changes; $I_z U^S \rightarrow I_y U^S$ and $U^I S_z \rightarrow U^I S_y$. During the time t_1, which is incremented as $n\Delta t_1$, $n = 1, 2, 3, \ldots$, $I_y U^S$ and $U^I S_y$ are modified because of evolution from the combined effects of chemical shift offset and scalar coupling. The effect of each can be calculated separately by noting that for the chemical shift offset S_y evolves as follows:

$$S_y(t_1) = S_y \cos(\Delta\omega_S t_1) + S_x \sin(\Delta\omega_S t_1) \qquad (12.2)$$

and U^I evolves under the influence of the scalar coupling as

$$U^I(t_1) \rightarrow U^I \cos(\pi J t_1) - \mathrm{i} I_z \sin(\pi J t_1) \qquad (12.3)$$

(remember, each component of the doublet is precessing by a differential of $\pm\pi J$ rad^{-1} relative to the chemical shift offset frequency). Considering the two precessional effects acting upon $U^I S_y$, the changes induced are as follows:

$$U^I S_y \xrightarrow{t_1, \Delta\omega_S} U^I S_y \cos(\Delta\omega_S t_1) + U^I S_x \sin(\Delta\omega_S t_1) \qquad (12.4)$$

$$\begin{aligned} &\xrightarrow{t_1, J} U^I S_y \cos(\Delta\omega_S t_1)\cos(\pi J t_1) \\ &\qquad (A) \\ &\quad - I_z S_x \cos(\Delta\omega_S t_1)\sin(\pi J t_1) \\ &\qquad (B) \\ &\quad + U^I S_x \sin(\Delta\omega_S t_1)\cos(\pi J t_1) \\ &\qquad (C) \\ &\quad + I_z S_y \sin(\Delta\omega_S t_1)\sin(\pi J t_1) \\ &\qquad (D) \end{aligned} \qquad (12.5)$$

The precession arising from a combination of chemical shift offset and scalar coupling has evolved $U^I S_y$ into four terms A, B, C, and D. Now the action of the second $\pi/2(j)$ pulse can be considered. (Note there will be, correspondingly, four terms generated from $I_y U^S$.) If the phase of the final $\pi/2$ pulse is set as $j = x$, each term whose origin was S_z is changed as follows:

$$\left.\begin{aligned} A &\rightarrow -U^I S_z \cos(\Delta\omega_S t_1)\cos(\pi J t_1),\ A'_x \\ B &\rightarrow -I_y S_x \cos(\Delta\omega_S t_1)\sin(\pi J t_1),\ B'_x \\ C &\rightarrow +U^I S_x \sin(\Delta\omega_S t_1)\cos(\pi J t_1),\ C'_x \\ D &\rightarrow -I_y S_z \sin(\Delta\omega_S t_1)\sin(\pi J t_1),\ D'_x \end{aligned}\right\} \qquad (12.6)$$

Terms A'_x and B'_x do not represent observable signal; one term is purely z magnetization while the other is a mixture of zero and double quantum coherence and is consequently unobservable. If the phase of the second pulse is set as $j = y$, the observable terms arise from

$$\left.\begin{aligned} &U^I S_y \cos(\Delta\omega_S t_1)\cos(\pi J t_1),\ A'_y \\ &\text{and} \\ &I_x S_z \cos(\Delta\omega_S t_1)\sin(\pi J t_1),\ B'_y \end{aligned}\right\} \qquad (12.7)$$

The significance of these terms will become apparent later.

12.2.2 COSY as a Two-Dimensional Experiment

One-dimensional NMR spectroscopy is well understood and can be explained using simple vectors. $U^I S_z$ receives a $\pi/2(x)$ pulse generating $U^I S_y \equiv (\alpha^I + \beta^I) S_y$ and this magnetization, because of precession in the laboratory frame, generates signals the frequency of which are separated by J Hz. The signals are sampled for a time $t_2 = m\Delta t_2$, $m = 1, 2, 3, \ldots$, yielding an observable spectral width $F_2 = 1/(2\Delta t_2)$ assuming quadrature detection. In 2D spectroscopy, a second time period is introduced during which the magnetization is modified advantageously for extra chemical structural information to be encoded. The spectral width in the second dimension F_1 is given by $1/(2\Delta t_1)$, again assuming quadrature detection. The values of m and n define the spectral resolution in the F_2 and F_1 dimensions, respectively. Double Fourier transformation of the data set yield peaks at coordinates (F_1, F_2) in frequency space.

For the COSY experiment with $i = j = x$, two signal groupings arise, one from C'_x and the other from D'_x. Consider firstly the signals arising from C'_x. Assuming that quadrature detection in F_2 is employed, the signals will be centered at $\Delta\omega_S/2\pi$ in the F_2 direction because they arise from the spin coherence $U^{\mathrm{I}}S_x \equiv (\alpha^{\mathrm{I}} + \beta^{\mathrm{I}})S_x$. The COSY signal will be 90° phase shifted compared with that arising from the standard pulse-and-collect experiment which is associated with the spin coherence $U^{\mathrm{I}}S_y$ for an x-phased excitation pulse. In the F_1 direction, the behavior is complex but can be readily calculated using the trigonometric identities $\cos x = (1/2)[\exp(\mathrm{i}x) + \exp(-\mathrm{i}x)]$ and $\sin x = (1/2\mathrm{i})\,[\exp(\mathrm{i}x) - \exp(-\mathrm{i}x)]$. For that component of the S doublet arising from the I eigenstate α^{I}, there will be two doublets either side of $F_1 = 0$, centered at $\pm\Delta\omega_S/2\pi$ in F_1. These arise from Fourier transformation of $\sin(\Delta\omega_S t_1)\cos(\pi J t_1)$ with respect to t_1. In F_1 the peaks occur at $(\Delta\omega_S/2\pi + J/2)$, $(\Delta\omega_S/2\pi - J/2)$ and $(-\Delta\omega_S/2\pi + J/2)$, $(-\Delta\omega_S/2\pi - J/2)$. There will be, as well, four corresponding peaks arising from the I eigenstate β^{I} yielding in total eight peaks. Note, no mention has been made concerning two-dimensional lineshapes. If the (F_1, F_2) plane (a contour map) were viewed from above, the eight peaks would appear as 'dots'.

The signals arising from D'_x are far more interesting. In the F_2 dimension they are centered at $\Delta\omega_I/2\pi$ and are generated by a signal arising from $-I_yS_z \equiv I_y(-\alpha^{\mathrm{S}} + \beta^{\mathrm{S}})$ by its evolution during t_2. (At $m = 0$, $-I_yS_z$ yields zero net signal, but during the t_2 evolution period $S_z \rightarrow [S_z\cos(\pi J t_2) - \mathrm{i}U^{\mathrm{S}}\sin(\pi J t_2)]$ giving rise to detectable magnetization.) Because the signals arise from correlated S_z magnetization, $S_z = (-\alpha^{\mathrm{S}} + \beta^{\mathrm{S}})$, they must be antiphase following the Fourier transformation. That is, the signals corresponding to α^{S} will be 180° phase shifted compared with those arising from β^{S}. Importantly, however, the signals are centered at $\pm\Delta\omega_S/2\pi$ in F_1, and specifically at $(\Delta\omega_S/2\pi + J/2)$, $(\Delta\omega_S/2\pi + J/2)$ and $(-\Delta\omega_S/2\pi + J/2)$, $(-\Delta\omega_S/2\pi - J/2)$. The salient features of this experiment are summarized in Figure 12.1.

The importance of this pulse sequence for structural chemistry should be now apparent. If there is J-coupling between two spins I and S there is a cross peak in the 2D spectrum arising from the spin coherence represented by the term D'_x centered at frequency coordinates in absolute units at $(\Delta\omega_S/2\pi,\ \Delta\omega_I/2\pi)$ in the (F_1, F_2) plane. There is

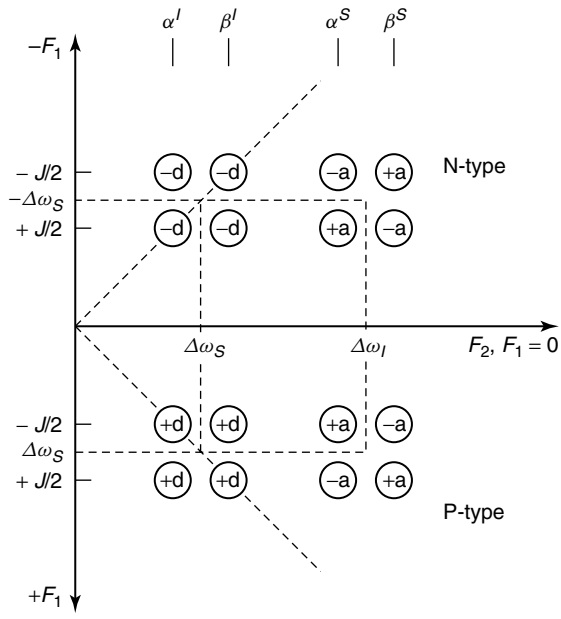

Figure 12.1. Theoretical COSY spectrum for two weakly coupled spins. The phases are illustrated by + or −, while the lineshapes are designated d (dispersion) and a (absorption). Only the peaks arising from spin S are shown; there are, as well, 16 peaks from spin I.

of course a cross peak (not shown in Figure 12.1) at $(\Delta\omega_I/2\pi,\ \Delta\omega_S/2\pi)$ as well. In total, the basic COSY experiment, $i = j = x$, yields 32 peaks in the 2D spectrum when applied to an I–S spin system. The two families of peaks are denoted as N-type or P-type.

The designation N and P is derived from the differences in the direction of precession during the t_1 and t_2 time periods. N means the direction is reversed or one the negative of the other. P means they are both of the same sign: positive. As the coherence transfer echo is usually detected (magnetic field inhomogeneity is refocused for this family of peaks), one axis of the 2D plot has frequency increasing left to right (F_2 direction) and decreasing bottom to top (F_1 direction). Thus, for the N-type peaks, the diagonal runs from left to right with a slope of 45° (see Figure 12.1). However, by software, one axis is usually reversed for visual display in order that chemical shifts decrease left to right and from bottom to top for display of the N-type peaks.

12.3 SIMPLIFICATIONS AND EXTENSIONS OF THE BASIC EXPERIMENT

12.3.1 Coherence Selection by Phase Cycling

Quadrature detection in the F_1 dimension is used to eliminate either the N- or P-type peaks. For N-type selection, the simplest phase cycle is to set $i = x$ and to generate data sets for $j = x$ and $j = y$. The data sets are subtracted during the complex Fourier transformation to yield quadrature detection[3] in F_1. This is simply understood by realizing that the complex data set when transformed generates the diagonal peaks arising now from the spin coherence:

$$\begin{aligned} C'_x - A'_x &= U^I S_x \sin(\Delta\omega_S t_1)\cos(\pi J t_1) \\ &\quad - U^I S_y \cos(\Delta\omega t_1)\cos(\pi J t_1) \\ &= U^I \cos(\pi J t_1)[S_x \sin(\Delta\omega_S t_1) \\ &\quad - S_y \cos(\Delta\omega_S t_1)] \\ &= -U^I \cos(\pi J t_1)[S_y \cos(\Delta\omega_S t_1) \\ &\quad - \mathrm{i} S_y \sin(\Delta\omega_S t_1)] \\ &= -U^I S_y \cos(\pi J t_1)\exp(-\mathrm{i}\Delta\omega_S t_1) \end{aligned} \tag{12.8}$$

A similar analysis for the cross peaks yields

$$D'_x - B'_y = -S_z I_x \sin(\pi J t_1)\exp(-\mathrm{i}\Delta\omega_S t_1) \tag{12.9}$$

If P-type selection is desired, the data sets generated from $j = x$ and $j = y$ are added during the transform. Usually, for even modern NMR spectrometers, if N-type peaks are to be selected, the simple phase cycle above, because of pulse imperfections, does not induce accurate suppression of the P-type family. The phase cycle needs to be extended to $i = x$; $j = x$, $-x$, y, $-y$ and the receiver $+,+$, $-,-$. Here, note that $C'_x = C'_{-x}$ and $D'_x = D'_{-x}$.

12.3.2 Coherence Selection using Pulsed Field Gradients

The modification to the COSY pulse sequence incorporating pulsed field gradients[4] is shown in Figure 12.2. The effect of the field gradient can be rationalized as follows.[5] A field gradient varies the angular precession of the I and S spins according to their spatial position. Consider the simplest type of spatial dependence arising from the application of a linear field gradient, for example, G_z. All spins in the plane defined by a z coordinate z_i have their Larmor frequency modified by an amount $(\Delta\omega_I + \Delta\omega)$ and $(\Delta\omega_S + \Delta\omega)$, respectively; $\Delta\omega = \gamma z_i G_z$. The gradient is applied for a short time τ_D on either side of the final $\pi/2$ pulse. The first gradient pulse modifies the spin coherence that gives rise to the diagonal peaks following the final $\pi/2$ pulse, $j = x$ to

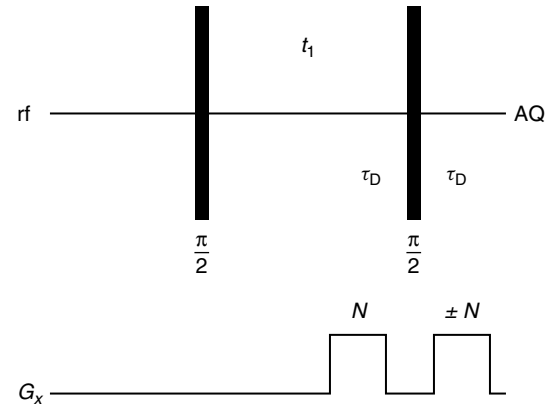

Figure 12.2. COSY pulse sequence incorporating field gradients for coherence selection.

$$\begin{aligned} &U^I S_x \cos(\pi J t_1)\sin(\Delta\omega_S t_1 + \Delta\omega\tau_D) \\ &\quad = \frac{1}{2\mathrm{i}} U^I S_x \cos(\pi J t_1)[\exp\{\mathrm{i}(\Delta\omega_S t_1 + \Delta\omega\tau_D)\} \\ &\qquad - \exp\{-\mathrm{i}(\omega_S t_1 + \Delta\omega\tau_D)\}] \end{aligned} \tag{12.10}$$

Application of a second equal gradient pulse having the same time integral as the first immediately before data acquisition yields evolution as:

$$\begin{aligned} &\frac{1}{4\mathrm{i}} U^I \cos(\pi J t_1)[S_+ \exp(\mathrm{i}\Delta\omega\tau_D) \\ &\quad + S_- \exp(-\mathrm{i}\Delta\omega\tau_D)] \times [\exp\{\mathrm{i}(\Delta\omega_S t_1 + \Delta\omega\tau_D)\} \\ &\quad - \exp\{-\mathrm{i}(\Delta\omega_S t_1 + \Delta\omega\tau_D)\}] \end{aligned} \tag{12.11}$$

The terms in which $\Delta\omega$, the gradient-induced offset, remains represent dephased magnetization. (Their linewidth will be such that they will yield unobservable signal provided G_z is sufficiently strong.) Thus, the detected signal is given by

$$\begin{aligned} &\frac{1}{4\mathrm{i}} U^I \cos(\pi J t_1)[-S_+ \exp(-\mathrm{i}\omega\Delta_S t_1) \\ &\quad + S_- \exp(\mathrm{i}\Delta\omega_S t_1)] \end{aligned} \tag{12.12}$$

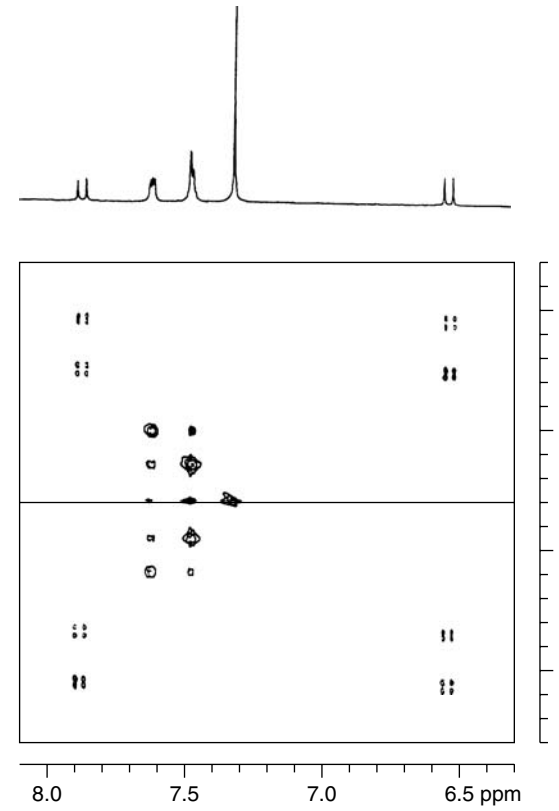

Figure 12.3. Contour plot of a normal COSY spectrum of 20 mM cinnamic acid in $CDCl_3$ obtained with one acquisition per t_1 increment. (No phase cycling has been employed.) A 512 × 2k data matrix with a spectral width of 1000 Hz in ω_1 and 2000 Hz in ω_2 was collected and zero filled once in ω_1 prior to 2D Fourier transformation. A simple pulse and acquire spectrum is plotted above the contour plot (see Ref. 5).

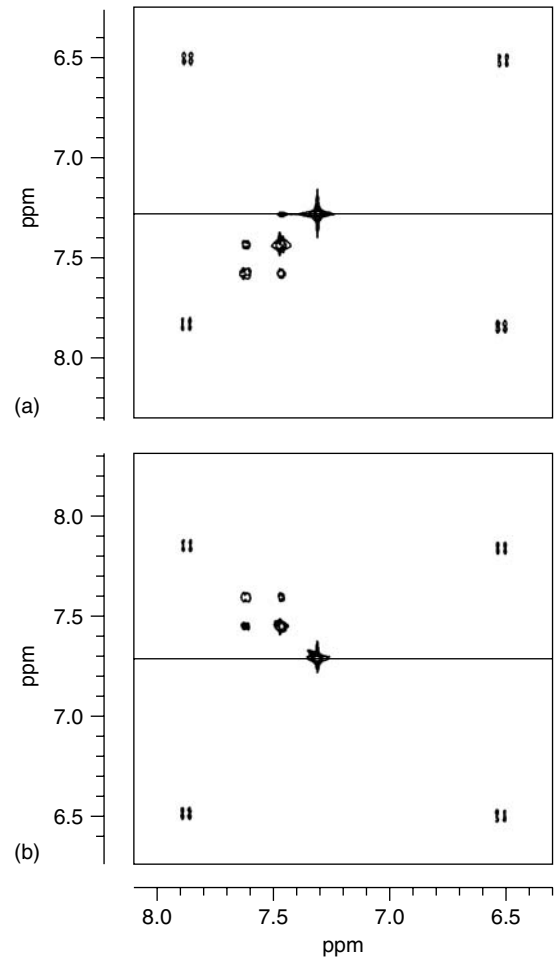

Figure 12.4. Contour plots of COSY spectra obtained using gradient pulses of the same sign and opposite sign, respectively. Note, the selection of the N- or P-type families of peaks. A single acquisition per t_1 increment was collected and data processed under conditions identical to those described in Figure 12.3 (see Ref. 5).

which reduces to

$$-\tfrac{1}{2}U^I S_y \cos(\pi J t_1) \exp(-\Delta\omega_S t_1) \qquad (12.13)$$

This again represents quadrature detection of S_y with respect to t_1 and again corresponds to N-type selection. Inverting the sign of the second gradient allows P-type selection. Single acquisition COSY, N-type selected and P-type selected using pulse field gradients are shown in Figure 12.3 and Figure 12.4, respectively.

12.4 OTHER NUANCES OF THE EXPERIMENT

The original experiment as proposed by Jeener has been explained above. Various facets and modifications, however, to this experiment have been published. Some are mentioned here to provide the interested reader with the references to probe further.

Note, that for N-type selection the sense of precession during t_1 is opposite to that for P-type selection. Thus, by analogy with the gradient selected COSY experiment, it is clear that for this peak family magnetic field inhomogeneity effects are refocused during t_2. The N-type peaks are called the coherence transfer echo; the P-type peaks the anti-echo.[6]

Because of finite linewidths in F_2, the lineshapes in the (F_1, F_2) plane are of interest. The lineshapes that will arise from the simple analysis (equation (12.6)) discussed above are 'phase-twisted'. More complex data analysis and phase cycling are required to remove the 2D spectral distortions that arise.[7]

The basic COSY pulse sequence has been modified to use double quantum filtering to increase the 2D spectral resolution.[1,8] Other modifications, at the expense of increasing the pulse sequence length, have been introduced to remove the antiphase character of the cross peaks.[9]

Attempts to introduce localization to the basic experiment have been published whereby the two COSY pulses have been made slice selective.[10] Only recently have gradient selective localized COSY experiments been demonstrated in vivo.[11]

REFERENCES

1. J. Jeener, AMPERE Summer School, Basko, Polje, Yugoslavia, 1971; W. P. Aue, E. Bartholdi, and R. R. Ernst, *J. Chem. Phys.*, 1976, **64**, 2229. For a good discussion also see H. Kessler, M. Gehnke, and C. Griesinger, *Angew. Chem., Int. Ed. Engl.*, 1988, **27**, 490.
2. Various constructions of product-operator algebra have been published, see R. R. Ernst, G. Bodenhausen, and A. Wokaun, *Principles of Nuclear Magnetic Resonance in One and Two Dimensions*, Clarendon Press, Oxford, 1987; F. J. M. van de Var and C. W. Hilbers, *J. Magn. Reson.*, 1983, **54**, 512; K. J. Packer and K. M. Wright, *Mol. Phys.*, 1983, **50**, 797; R. M. Lynden-Bell, J. M. Bulsing, and D. M. Doddrell, *J. Magn. Reson.*, 1983, **55**, 128.
3. D. J. States, R. A. Haberkorn, and D. J. Ruben, *J. Magn. Reson.*, 1982, **48** 286; D. Marion and K. Wüthrich, *Biochem. Biophys. Res. Commun.*, 1983, **113**, 967.
4. P. Barker and R. Freeman, *J. Magn. Reson.*, 1985, **64**, 334.
5. I. M. Brereton, S. Crozier, J. Field, and D. M. Doddrell, *J. Magn. Reson.*, 1991, **93**, 54.
6. K. Nagayama, K. Wüthrich, and R. R. Ernst, *Biochem. Biophys. Res. Commun.*, 1979, **90**, 305.
7. J. Keeler and D. Neuhaus, *J. Magn. Reson.*, 1985, **63**, 454.
8. A. A. Maudsley, A. Wokaun, and R. R. Ernst, *Chem. Phys. Lett.*, 1979, **55**, 9; A. Bax, P. De Jong, A. F. Mehlkopf, and J. Smidt, *Chem. Phys. Lett.*, 1980, **69**, 567.
9. A. Kumar, R. V. Hosur, and K. Chandrasekhar, *J. Magn. Reson.*, 1984, **60**, 143; S. Talluri and H. A. Scherager, *J. Magn. Reson.*, 1990, **86**, 1.
10. S. J. Blackband, K. A. McGovern, and I. J. McLennan, *J. Magn. Reson.*, 1988, **79**, 184. See also, Y. Cohen, L.-H. Chang, L. Litt, and T. L. James, *J. Magn. Reson.*, 1989, **85**, 203; G. C. McKinnon and P. Bosiger, *Magn. Reson. Med.*, 1988, **6**, 334.
11. I. M. Brereton, G. J. Galloway, S. E. Rose, and D. M. Doddrell, *Magn. Reson. Med.*, 1994 **32**, 251.